Journal of Cellular Biochemistry 88:372–380 (2003)

Inhibitors of Vitamin D Hydroxylases: Structure–Activity Relationships

Inge Schuster,[1]* Helmut Egger,[2] Peter Nussbaumer,[2] and Romano T. Kroemer[3]

[1]Institute of Pharmaceutical Chemistry, University Vienna, Althanstraße 15, A-1090 Wien, Österreich
[2]Novartis Research Institute, Brunnerstraße 59, A-1235 Wien, Österreich
[3]Pharmacia, Viale Pasteur 10, 20014 Nerviano, Italy

Abstract Aiming at new drugs to efficiently treat diseases, in which either increased or decreased levels of active vitamin D are desirable, we have designed some 400 structurally different azole-type inhibitors and examined their capacity to selectively block vitamin D metabolism by CYP24 or synthesis by CYP27B, in human keratinocytes. Based on resulting data, we built pharmacophore models of the active sites using commercial software. The overlay of potent selective compounds indicated similar docking modes in the two-substrate pockets and allowed for identification of bioactive conformations. Superimposing these bioactive conformations with low energy conformers of 25(OH)D_3 suggested that the substrate-mimicked by strong inhibitors in size, shape and lipophilic character-binds to both enzymes in 6s-*trans* configuration. Pharmacophoric models implied a similar geometry of the substrate sites, nevertheless specific features of CYP24 and CYP27B could be defined. Bulky substituents in α-position to the azole caused selectivity for CYP24, whereas bulky substituents in β-position could result in selectivity for CYP27B. Moreover, studies with small sterically restricted inhibitors revealed a probable location of the 3-OH-group of 25(OH)D_3 in CYP27B. In the absence of crystal structures, our inhibitors are valuable tools to model and understand the active sites of vitamin D hydroxylases, resulting in the design of powerful, selective therapeutics. J. Cell. Biochem. 88: 372–380, 2003. © 2002 Wiley-Liss, Inc.

Key words: CYP24; CYP27B; inhibition; pharmacophoric model; active site

The important role of vitamin D in many physiological and pathological processes makes the enzymes controlling its levels attractive new targets for the development of drugs. 25-Hydroxyvitamin D-1α-hydroxylase (CYP27B), the key enzyme in the synthesis of the hormonally active form 1,25$(OH)_2D_3$, is expressed in kidney and a wide range of extrarenal tissues, including various types of tumors [Dusso et al., 1994; Garcion et al., 2002]. In practically all tissues, 1,25$(OH)_2D_3$ rapidly induces expression of 24-hydroxylase (CYP24), a multicatalytic enzyme, which attacks the vitamin D side chain in successive oxidations and eventually terminates hormone action [Akiyoshi-Shibata et al., 1994, Beckman et al., 1996]. Consequently, by slowing down hormone metabolism and depletion, inhibitors of CYP24 raise local levels and lifetime of biologically active metabolites and, thereby extent and duration of hormone action [Schuster et al., 2001a]. For a highly reduced potential risk of calcemic side effects, CYP24 inhibitors could become a valuable alternative to hormone substitution therapy [Schuster et al., in press]. On the contrary, inhibitors of CYP27B will suppress hormone synthesis and, thereby exert beneficial actions in hypercalcemic conditions.

CYP27B and CYP24 are members of the very large cytochrome P450 (CYP) superfamily [Omdahl et al., 2001]. Both enzymes are integrally located in the inner mitochondrial membrane and as for almost all mammalian CYPs structural information from X-ray crystallography or NMR analyses is still missing. Inhibitors of these enzymes offer an indirect method to probe the topography of the active sites.

Especially, valuable, powerful inhibitors of CYP enzymes are found in a class of compounds, termed azoles, which directly bind to the

*Correspondence to: Inge Schuster, PhD, Institute of Pharmaceutical Chemistry, University Vienna, A-1090 Wien, B-Althanstasse 15, Austria.
E-mail: inge@tbi.univie.ac.at

Received 6 September 2002; Accepted 9 September 2002
DOI 10.1002/jcb.10365

prosthetic heme iron via a lone electron pair from a heterocyclic nitrogen and, additionally interact with other sites in the binding pocket [Poulos, 1988]. Accordingly, these bi-functional compounds block both oxygen binding and activation at the heme iron as well as substrate accommodation in the active site. The two types of interactions also stabilize the enzyme-inhibitor complex, resulting in high-affinity binding. Azole-type inhibitors were exploited for molecular modeling of the active site of various CYPs and, importantly, gave rise to successful drugs, used in numerous indications ranging from fungal infections to steroid hormone dependent cancer [Ahmed, 1999; Brodie, 2002]. The antifungals ketoconazole, clotrimazole, itraconazole, and fluconazole are prominent examples of azole-type drugs. However, these and most other azoles bear a substantial risk to cause selectivity problems, since docking at the heme iron of one CYP does not rule out docking at the heme of a different CYP, if the active site is sufficiently large.

Aiming at new therapeutic agents to treat vitamin D responsive diseases, especially in skin, we have designed and synthesized a large set of structurally different azole-type compounds. These compounds were examined for their capacity to selectively block vitamin D metabolism by CYP24 (24-hydroxylase) or synthesis by CYP27B (1α-hydroxylase) in primary cultures of human keratinocytes as model system [Schuster et al., 2001a]. In this report, we describe some of the structure–activity relationships resulting from analyses of the inhibition data and show pharmacophore models of the active sites of CYP24 and CYP27B, based on the overlays of representative sets of strong, selective inhibitors.

DESIGN AND TESTING OF INHIBITORS

In total, we examined the potential of some 400 azole compounds to inhibit CYP24 and CYP27B. Besides a few standards from other companies (e.g., ketoconazole, clotrimazole, fluconazole, itraconazole, liarozole), all other azoles were specifically designed and synthesized in Novartis. The broad synthesis program included systematic variation of the azole group (e.g., imidazoles, triazoles, pyridine) and substitution of the side chains extending at the C-atoms in α- and/or β-position to the azole group (with short and long, sterically restricted and flexible side chains) with a representative large variety of substituents [Schuster et al., in press]. Since many compounds comprised chiral centers, in most cases, pure R- and/or S-enantiomers were produced by chiral synthesis or chromatographic separation. Results on potency and selectivity of compounds (for CYP24) were continuously fed into the design of new improved inhibitors and used for pharmacophore modeling (see below).

Inhibition data were produced by a protocol, modified after Bikle et al. [1986] and published in detail elsewhere [Schuster et al., 2001a]. In short, we incubated confluent cultures of human keratinocytes isolated from adult skin (mainly obtained from cosmetic surgery and mammary reduction) in serum-free keratinocyte growth medium (KGM, Clonetics) with physiological levels of [n26,27-^{3}H]-25(OH)D_3 (10–20 nM; 15–17 Ci/mmol, Amersham) in absence and presence of test compounds (0–10 μM). Inhibition of CYP27B-activity was determined after 1 h incubation from the (reduced) rate of substrate conversion to 1-hydroxylated metabolites (1,25$(OH)_2D_3$ + 1,25$(OH)_2$-3-epi-D_3). Inhibition of CYP24 was assessed after 2–3 h incubation at the "initial stage" of CYP24-induction by endogenously produced 1,25$(OH)_2D_3$ from the rate of total 24-hydroxylation, taking into account the number of attacks required for each 24-oxidized product. Formation of individual metabolites was followed by sensitive high performance liquid chromatography of organic incubation extracts on Zorbax-Sil (non-linear gradient 97:3–85:15% n-hexane: 2-propanol), using a highly sensitive online radioactivity detector (Radiomatic 500TR, Canberra) to detect and quantify radioactive peaks, which were assigned to chemical structures by matching with co-chromatographed authentic standards (kindly provided by GS Reddy, Brown University, Providence, RI). IC_{50}-values were determined from plots of enzyme activity versus inhibitor concentration, using the GRAFIT-IC50-software (Grafit 4.12, Erithacus).

Of the approximately 400 tested compounds, more than 60 showed high potency (IC_{50} in the low to medium nanomolar concentration range) and selectivity (up to two orders of magnitude) for either CYP24 or CYP27B. Most of these compounds had highly lipophilic character and semi-rigid structures. Table I displays few examples of strong selective inhibitors. For comparison, ketoconazole, a potent inhibitor of both

TABLE I. Examples of Potent Selective Inhibitors of CYP27B and CYP24

Compound	Chemical structure	IC_{50} [nM]		Selectivity for	
		CYP27B	CYP24	CYP27B	CYP24
SDZ-88357 (racemic mixture)	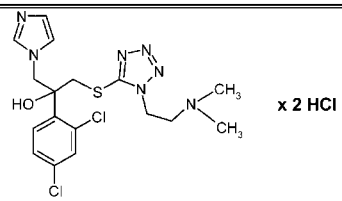	60.2 (6.5)	> 10000	> 166	< 0.006
SDZ-283251 (racemic mixture)	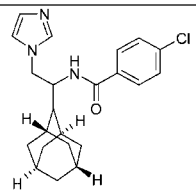	710.9 (86.7)	>>20000	> 30	< 0.03
SDZ-284971	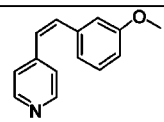	78.8 (10.7)	≥ 10000	≥ 126.9	≤ 0.008
Ketoconazole	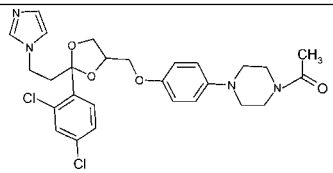	28.3 (7.5)	126.0 (1.8)	4.45	0.22
VID400 (R)	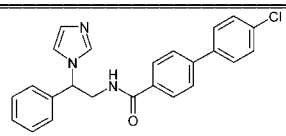	616.2 (113.2)	15.2 (3.5)	0.024	40.5
SDZ-285428 (S)		353.2 (60.9)	36.2 (8.3)	0.068	14.7
SDZ-286907 (R)	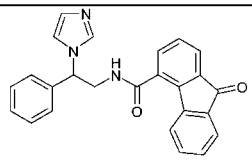	1696.9 (421.9)	34.9 (6.85)	0.021	48.6
SDZ-287871 (R)	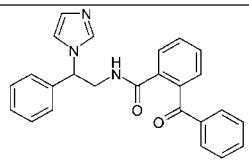	1271.6 (326,5)	29.9 (8.5)	0.024	42.5
VAB636 (R)	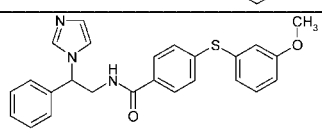	266.1 (32.5)	5.08 (0.31)	0.019	52.3

Inhibition studies were done in human keratinocyte cultures, as described in the text. IC_{50}-values (with SD in parentheses), determined with the GRAFIT IC50-4 parameter software (Graft 4.12, Erithacus), are means of triplicates.

enzymes with weak selectivity for CYP27B, is included.

PHARMACOPHORE METHOD

Pharmacophore models are built by superimposing ligands, substrates, or inhibitors of a protein, matching chemically similar groups of these effectors. From this overlay, indirect information on the shape, size, and electrostatic properties of the active site of proteins is gained [DeGroot and Ekins, 2002]. We have used a program called DISCO (DIStance COmparison,

Tripos), which is a module of the computational SYBYL software and has been described by Martin et al., [1993]. In a representative set of active compounds, this fast method simultaneously identifies the bioactive conformation and the pharmacophore pattern.

Since our major goal was to identify azole compounds with improved selectivity (for CYP24), we were especially interested in relevant structural differences between the active sites of CYP24 and CYP27B. Therefore, the collection of compounds used for modeling consisted of inhibitors, which beyond high potency, widely differing substitution pattern and reduced flexibility, also showed selectivity for the one or the other enzyme. In a first series, six inhibitors were selected for each enzyme; SDZ-285428 (Table I) served as template for CYP24 ligands and SDZ-89382 (not shown) as template of CYP27B. The inhibitors were linked with their azole-N3 to the heme iron in a distance of 2 Å [Scheidt et al., 1987], thereby reducing the conformational space. For each compound low-energy conformations were generated (by the Systematic-Search procedure of SYBYL), aiming at covering the entire (reduced) conformational space, and pharmacophoric properties (e.g., charge, hydrogen bonds, hydrophobicity) automatically identified either on the molecule or on projections from the molecules to H-bond donors and acceptors or charged groups in the binding pocket. Using a clique-detection algorithm [Martin et al., 1993], the common three-dimensional (3D) arrangement of features was identified and 3D pharmacophoric models were generated.

PHARMACOPHORIC MODELS

From some 80 pharmacophoric models generated for each enzyme, the model with the best alignment concerning the "azole"-"azole-donor points" and the hydrophobic regions was selected. Figure 1A,D display these models, each of them comprising two (large) hydrophobic areas (roughly indicated as grey-shaded area), at slightly differing distances from the azole. The overlay of the tested azole-inhibitors (Fig. 1B,E) showed a good geometrical fit, indicating a similar docking mode in the active pocket.

We also tentatively superimposed the bioactive conformation of inhibitors with low energy conformers of the substrate $25(OH)D_3$, assuming a similar geometric orientation of the site of attack (i.e., the C-1α-bond in CYP27B and the C-24 (R)-bond in CYP24) to the heme iron as described from crystal structures of CYP-substrate complexes (e.g., the orientation of the 5-exo-C-bond of camphor in CYP101 [Poulos, 1988]). Figure 1C tentatively superimposes $25(OH)D_3$ with a conformationally restricted inhibitor (SDZ-880014) in the hypothetical CYP27B site, Figure 1F with the template SDZ-285428 in the CYP24 site. In both enzymes, the overlays point to: (a) substrate binding might prefer the extended 6s-*trans* configuration, (b) strong inhibitors mimic the substrate in size and shape.

Importantly, the pharmacophoric models indicate a similar geometry of the substrate binding pockets in CYP27B and CYP24. As a result, powerful inhibitors of one enzyme might bind to the other enzyme in a comparable, strong manner. In fact, the majority of azole-compounds identified as strong inhibitors in our model systems, exhibited low or lacking selectivity for one of the enzymes, as exemplified with ketoconazole (Table I). However, from visual examination of the large collection of inhibition data, we were able to define specific criteria of CYP27B and CYP24, which could be valuable in the design of improved compounds. Two of these features will be described in the following sections.

SPECIFIC SITE IN CYP27B

We tested inhibition of CYP27B with three sets of small, closely related compounds, comprising a pyridyl-nitrogen as ligand to the heme iron (Fig. 2). The pyridine was linked in C-4 or C-3 to a phenyl-vinyl- or phenyl-ethyl residue, substituted with one or two methoxy-groups in *m*-position. With C-4 substituted compounds, inhibition of CYP27B depended on the stereochemistry at the central double bond. The *trans*-isomers (a,d) exhibited only weak inhibitory capacity ($IC_{50} = 3.5–12.5$ μM), whereas the *cis*-isomers (b,e) strongly blocked the enzyme ($IC_{50} = 0.08–0.12$ μM; Fig. 2A). Saturation of the double bond (c,f) resulted in a comparably strong interaction with the enzyme, indicating that the flexible molecule might have adopted the conformation of the rigid *cis*-isomer. In case of the 3-substituted pyridines (g–i), the preference for the *cis*-isomer was lost and all compounds interacted only weakly with the enzyme.

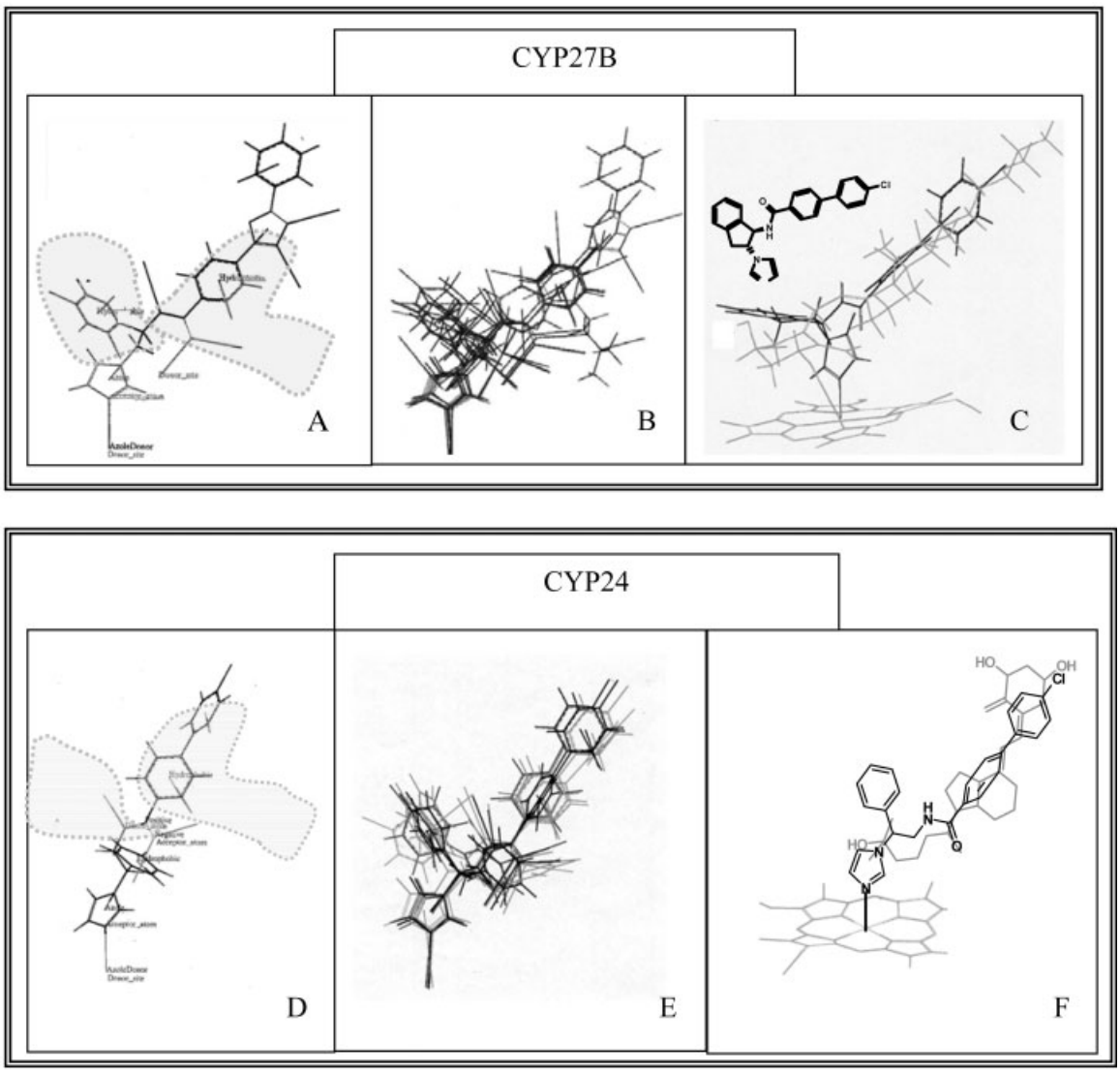

Fig. 1. Pharmacophoric models. **A**,**D**: ''Best'' models of CYP27B (A) and CYP24 (D) with hydrophobic regions indicated as light-grey areas. **B**,**E**: Representation of azole-type inhibitors superimposed in pharmacophoric conformations. **C**,**F**: Overlay of the sterically restricted compound SDZ-880014 (C) and the template SDZ-285-428 (F) with a conformer of the substrate 25(OH)D_3, assuming a similar geometric orientation of the C-1 α-bond in CYP27B (C) and of the C-24 (R)-bond in CYP24 (F) as the 5-exo-C-bond of camphor in CYP101 [Poulos, 1988].

When linked to the heme iron with the pyridyl-nitrogen, the overlay of the C-4 substituted *trans*-isomer (a) with the C-3 substituted *cis*-isomer (h) revealed an analogous adjustment of both compounds, but a different accommodation of the C-4 substituted *cis*-isomer (B).

Obviously, the 3-methoxy group played a decisive role in binding. Superimposing the strong inhibitor *cis*-4-[2-(3-methoxy-phenyl)-vinyl]-pyridine (b) with a conformer of the substrate 25(OH)D_3 showed that the 3-methoxy-group of the inhibitor was positioned close to the 3-OH-group of the substrate (C). Therefore, we hypothesize that in this molecule the CH_3O-group might interact by hydrogen bonding with the H-bond donor site that is normally required to fit the substrate via the 3β-hydroxy group in the binding pocket. Binding to this site in addition to the heme iron results in a strong interaction, whereas the *trans*-isomer and the C-3 substituted compounds displaying attachment to the heme iron only, exert by two orders of magnitude weaker binding. A second methoxy group in the phenyl ring did not confer to stabilization of the complex.

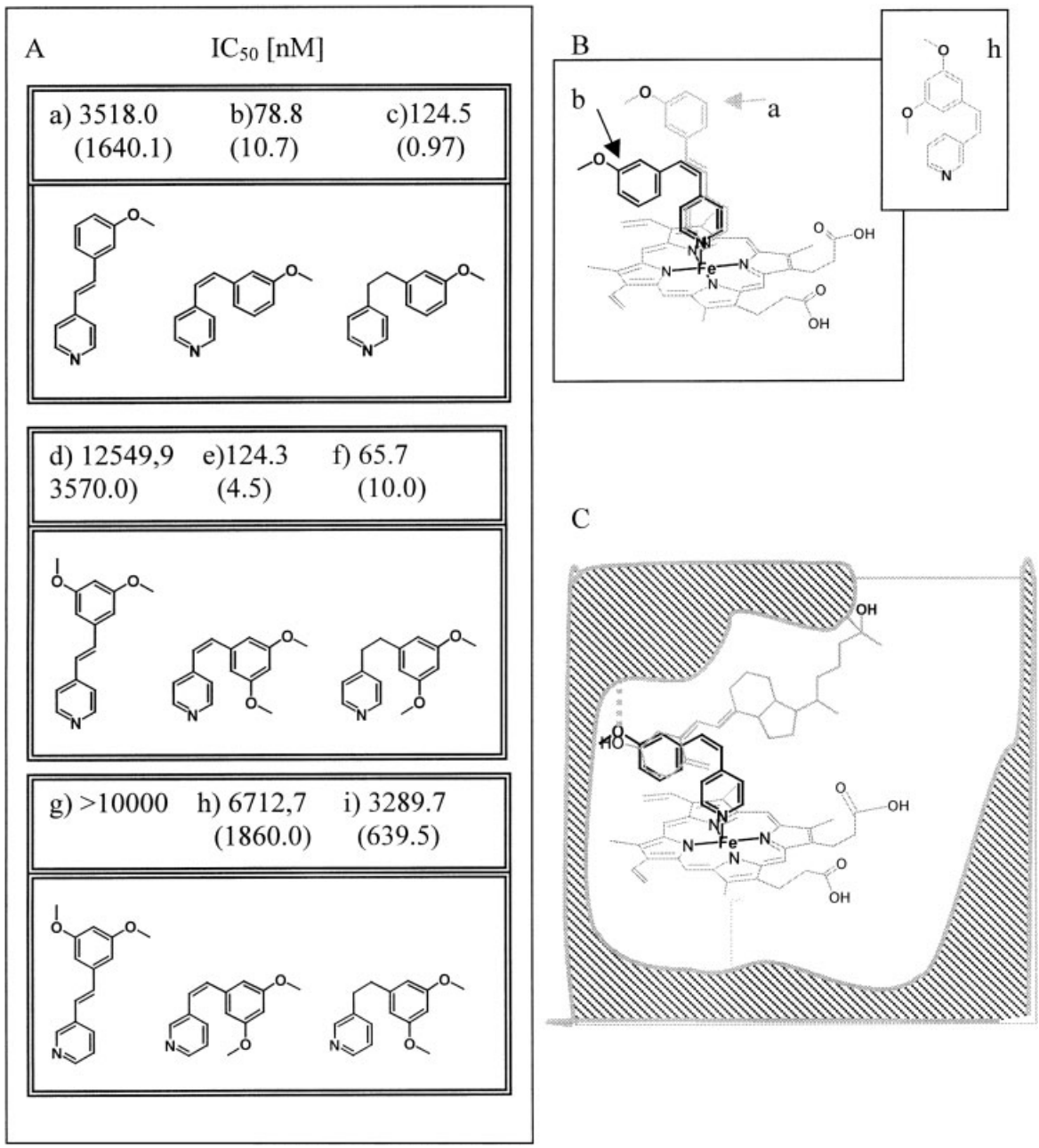

Fig. 2. Inhibition of CYP27B with C-4 and C-3 substituted pyridines. **A**: Chemical structures and IC_{50}-values. **B**: Overlay of the *trans*-and *cis*-form of 4-[2-(3-methoxy-phenyl)-vinyl]-pyridine attached with the pyridine nitrogen to the heme iron. The *cis*-form of the 3-substituted compound (h, insert) adopts a similar conformation as a. **C**: Hypothetical active site of CYP27B: Overlay of *cis*-4-[2-(3-methoxy-phenyl)-vinyl]-pyridine with a conformer of the substrate 25(OH)D_3, assuming a similar geometric orientation of the C-1α-bond as the 5-exo-C-bond of camphor in CYP101 [Poulos, 1988]. The 3-methoxy-group of the inhibitor lies close to the 3-OH-group of the substrate and may interact with its respective binding site (dotted line) and, thereby stabilize the binding. (For simplicity, overlays of inhibitors and substrate are displayed in 2D-mode.)

Using the ACD/3D-software (Advanced Chemistry Development Inc, Toronto, Canada), we calculated a distance between the oxygen of (b) and its pyridine nitrogen of 7.8 Å (depending on the twist between the two ring systems), corresponding to 8.8 Å between the oxygen and the heme iron (at a distance N-Fe of 2 Å [Scheidt et al., 1987]). This distance might reflect the separation between the heme iron and the 3β-hydroxy group of the natural substrate.

The described compounds are weak inhibitors of CYP24 ($IC_{50} > 10$ μM, data not shown).

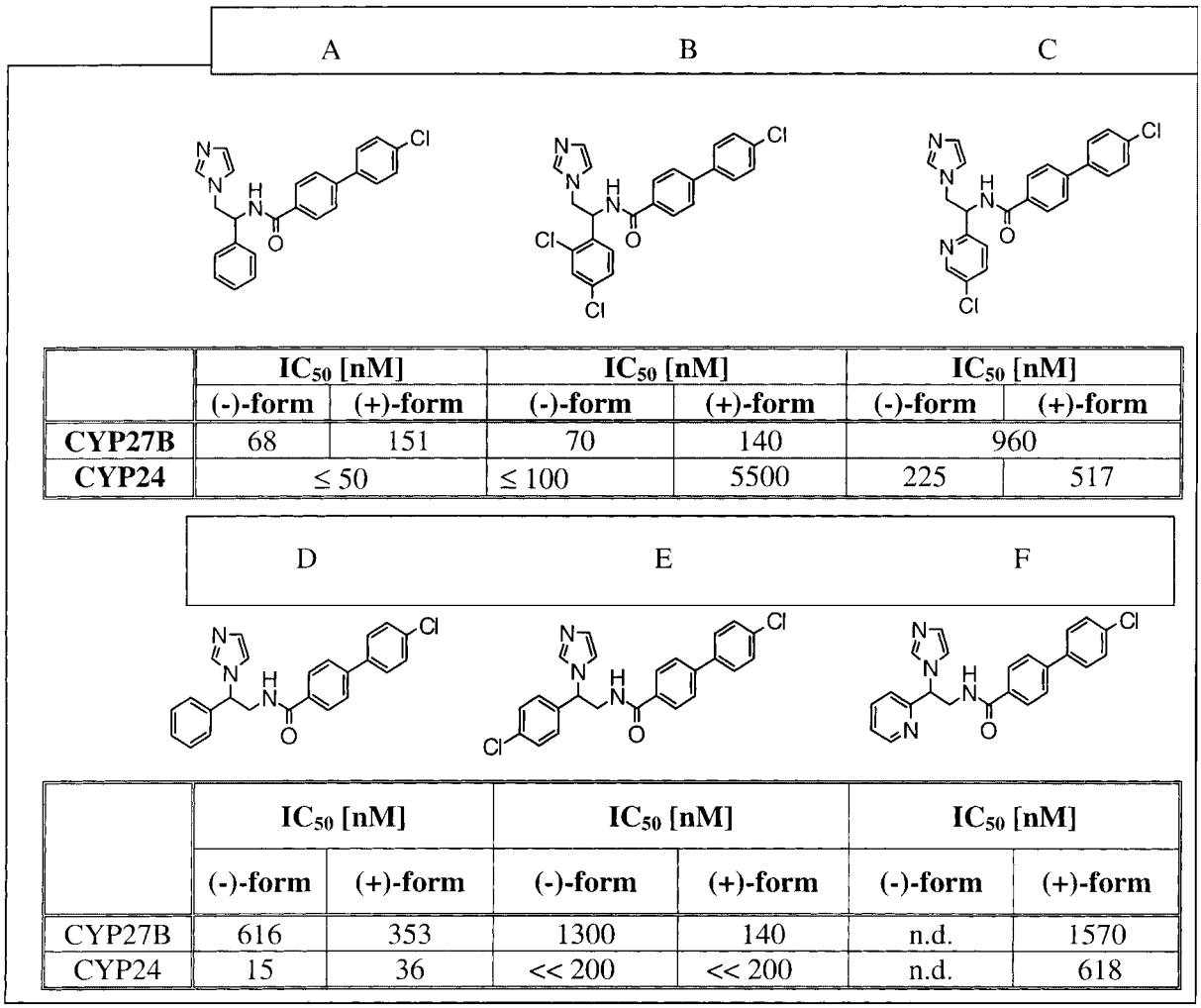

	IC_{50} [nM]		IC_{50} [nM]		IC_{50} [nM]	
	(-)-form	(+)-form	(-)-form	(+)-form	(-)-form	(+)-form
CYP27B	68	151	70	140	960	
CYP24	≤ 50		≤ 100	5500	225	517

	IC_{50} [nM]		IC_{50} [nM]		IC_{50} [nM]	
	(-)-form	(+)-form	(-)-form	(+)-form	(-)-form	(+)-form
CYP27B	616	353	1300	140	n.d.	1570
CYP24	15	36	<< 200	<< 200	n.d.	618

Fig. 3. Criteria for CYP24 selectivity, chemical structures, and IC_{50}-values of a representative series of related imidazole derivatives. IC_{50}-values determined in primary cultures of human keratinocytes as described are means of triplicates.

Therefore, compounds like *cis*-4-[2-(3-methoxyphenyl)-vinyl]-pyridine and its saturated counterpart could become valuable leads in the design of powerful, selective inhibitors of CYP27B.

SELECTIVITY CRITERIA FOR CYP24

As shown from similar pharmacophoric models, many strong inhibitors of CYP27B could also nicely fit into the active pocket of CYP24 and massively block this enzyme too. Figure 3 displays a representative series of closely related imidazole derivatives, which reveal some criteria for achieving selectivity for CYP24.

In our test system, compound A (4′-chloro-*N*-[2-(1*H*-imidazol-1-yl)-1-phenylethyl]-1,1′-biphenyl-4-carboxamide) worked as an equivalent, potent inhibitor of both enzymes. However, when phenyl-substitution switched from position 1 to 2 (compound D: 4′-chloro-*N*-[2-(1*H*-imidazol-1-yl)-2-phenylethyl]-1,1′-biphenyl-4-carboxamide; VID400 (−) and SDZ-285428 (+); see Table I), strong inhibition of CYP24 was maintained or even increased, however, binding to CYP27B became substantially weakened. A comparable characteristic was noticed with chlorine-substituted analogs. Strong inhibition of CYP27B by compound B was indistinguishable from inhibition by compound A, in both cases showing preference for the (−)-form. Switching phenyl-substitution from position 1 to 2 led to compounds like compound E with decreased affinity to CYP27B and high affinity to CYP24.

Similar data obtained with a wide variety of substituents, including (substituted) α-,

β-napthyls, -chinolins, etc., confirmed that selectivity for CYP24 could be achieved by bulky substituents in α-position to the azole. In contrast, bulky substituents in β-position to the azole (position 2) could result in selectivity for CYP27B (e.g., (+)-isomer of compound B, adamantyl-group (in SDZ 283251, Table I) etc.).

A further series of imidazole derivatives, comprising a pyridine substituent, revealed (weak) selectivity for CYP24, independent on the position of the pyridyl-group (e.g., compound C and F). These compounds were much less potent than corresponding phenyl counterparts, however, could offer important structural hints for the design of selective compounds.

CONCLUSIONS AND OUTLOOK

Inhibition of cytochromes P450, in particular of lanosterol demethylase (CYP51), aromatase (CYP19), and 17α-hydroxylase/17,20-lyase (CYP17), emerged as successful strategies to treat a wide range of diseases, ranging from fungal infections to hormone-dependent diseases, including cancer [Lamb et al., 1997, Ahmed, 1999, Brodie, 2002]. Since crystal structures of (almost all) eukaryotic CYPs are not yet available, inhibitor studies have also been used for modeling the active sites of major CYPs involved in drug metabolism as well as in steroid synthesis [Ahmed and Davis, 1995, Ekins et al., 2001, DeGroot and Ekins, 2002].

Vitamin D hydroxylases can be regarded as new promising targets for CYP inhibitors, since they offer therapeutic strategies applicable in a wide variety of diseases, in which either increased or decreased levels of (endogenous) hormonally active vitamin D are desirable [Schuster et al., in press]. Aiming at new drugs, we have designed some 400 structurally different azole-type inhibitors and examined their capacity to selectively block vitamin D metabolism by CYP24 or synthesis by CYP27B, using human keratinocytes as model system [Schuster et al., 2001a; Schuster et al., in press]. Besides profiling some of these compounds for therapeutic applications (e.g., VID400), we have used selective inhibitors as valuable novel tools to explore principles in the regulation of the vitamin D system, which were not amenable before [Schuster et al., 2001b]. Moreover, we exploited inhibition data to model the active sites of the enzymes, for which direct as well as indirect information on their tertiary structure is still missing.

The present report describes pharmacophoric models of the active sites of CYP24 and CYP27B, generated with the modeling software DISCO (Tripos) from the overlay of energy-minimized conformers of a representative set of strong and selective inhibitors, including conformationally restricted compounds. Common characteristics of both active sites were a similar large size, the presence of (at least) two hydrophobic regions and the likely accommodation of the substrate $25(OH)D_3$ in the extended 6s-*trans* configuration (Fig. 1). Specific differences were detected in the location of the hydrophobic regions, which allowed substitution with large bulky groups in C-α-position to the azole in CYP24 but not in CYP27B (Fig. 3D,E). On the contrary, large bulky groups in C-β-position to the azole raised the selectivity for CYP27B (Table I). An important selectivity criterion of CYP27B was recognized from its inhibition by a series of small *cis-trans*-isomers, comprising a *m*-methoxy-phenyl-vinyl residue linked to pyridine (Fig. 2). Up to 100-fold increased inhibition with the *cis*-isomers pointed to a specific binding in the pocket. Alignment of the compound with $25(OH)D_3$ gave a plausible explanation, namely hydrogen bonding of the CH_3O-group with the H-bond donor site, which fits $25(OH)D_3$ via its 3β-hydroxy group in the binding pocket.

For the sake of brevity, this report does not show further details on structural characteristics, exclusion, and selectivity criteria, which we obtained from our large sets of homogenous inhibition data (to be published elsewhere). It is obvious that these data offered an excellent basis for pharmacophore-modeling and 3D-quantitative structure–activity relationship (QSAR) studies, especially using CoMFA (comparative molecular field analysis). Since resulting information was continuously fed into the design of new inhibitors with improved selectivity, the "shape space" covered by the overall ensemble of compounds may be used to give a dynamic image of the active sites. These analyses together with homology modeling of the active sites are still in progress.

REFERENCES

Ahmed S. 1999. A novel molecular modelling study of inhibitors of the 17α-hydroxylase component of the enzyme system 17α-hydroxylase/17-20-lyase ($P450_{17\alpha}$). Bioorg Med Chem 7:1487–1496.

Ahmed S, Davis PJ. 1995. Molecular modelling of inhibitors of aromatase—A novel approach. Bioorg Med Chem Lett 5:1673–1678.

Akiyoshi-Shibata M, Sakaki T, Ohyama Y, Noshiro M, Okuda K, Yabusaki Y. 1994. Further oxidation of hydroxycalcidiol by calcidiol-24-hydroxylase: A study with the mature enzyme expressed in *Escherichia coli*. Eur J Biochem 224:335–343.

Beckman M, Tadikonda P, Werner E, Prahl JM, Yamada S, DeLuca HF. 1996. Human 25-hydroxyvitamin D_3-24-hydroxylase, a multicatalytic enzyme. Biochemistry 35: 8465–8472.

Bikle DD, Nemanic MK, Whitney JO, Elias PM. 1986. Neonatal human foreskin keratinocytes produce 1,25-dihydroxyvitamin D_3. Biochemistry 25:1545–1548.

Brodie A. 2002. Aromatase inhibitors in breast cancer. Trends Endocrinol Metab 13:61–65.

DeGroot MJ, Ekins S. 2002. Pharmacophore modelling of cytochromes P450. Adv Drug Deliv Rev 54:367–383.

Dusso A, Brown A, Slatopolsky E. 1994. Extrarenal production of calcitriol. Semin Nephrol 14:144–155.

Ekins S, DeGroot MJ, Jones JP. 2001. Pharmacophore and three-dimensional quantitative structure activity relationship methods for modelling cytochrome P450 active sites. Drug Metab Dispos 29:936–944.

Garcion E, Wion-Barbot N, Montero-Menei CN, Berger F, Wion D. 2002. New clues about vitamin D functions in the nervous system. Trends Endocrinol Metab 13:100–105.

Lamb DC, Kelly DE, Baldwin BC, Gozzo F, Boscott P, Richard WG, Kelly SL. 1997. Differential inhibiton of *Candida albicans* CYP51 with antifungal stereoisomers. FEMS Microbiol Lett 149:25–30.

Martin YC, Bures MG, Danaher EA, DeLazzer J, Lico I, Pavlik PA. 1993. A fast new approach to pharmacophore mapping and its application to dopaminergic and bezodiazepine agonists. J Comput Aided Mol Des 7:83–102.

Omdahl JL, Bobrovnikova EA, Choe S, Dwivedi PP, May BK. 2001. Overview of regulatory cytochrome P450 enzymes of the vitamin D pathway. Steroids 66:381–389.

Poulos TL. 1988. Cytochrome P450: Molecular architecture, mechanism, and prospects for rational inhibitor design. Pharm Res 5:67–75.

Scheidt RW, Osvath SR, Lee YJ. 1987. Crystal and molecular structure of bis(imidazole)(meso-tetraphenylporphinato)iron(III) chloride. A classic molecule revisited. J Am Chem Soc 109:1958–1963.

Schuster I, Egger H, Bikle D, Herzig G, Reddy GS, Stuetz A, Stuetz P, Vorisek G. 2001a. Selective inhibition of vitamin D hydroxylases in human keratinocytes. Steroids 66:409–422.

Schuster I, Egger H, Astecker N, Herzig G, Schüssler M, Vorisek G. 2001b. Selective inhibitors of CYP24: Mechanistic tools to explore vitamin D metabolism in human keratinocytes. Steroids 66:451–462.

Schuster I, Egger H, Herzig G, Reddy GS, Vorisek G. Combinations of vitamin D metabolites with selective inhibitors of vitamin D metabolism. Rec Res Cancer Res (in press).